Cosmic ray studies with KASCADE-Grande

M. Brüggemann[¶], W.D. Apel[*], F. Badea[*], K. Bekk[*], A. Bercuci[†], M. Bertaina[‡], J. Blümer[*], H. Bozdog[*], I.M. Brancus[†], P. Buchholz[¶], A. Chiavassa[‡], F. Cossavella[§], K. Daumiller[*], F. Di Pierro[‡], P. Doll[*], R. Engel[*], J. Engler[*], P.L. Ghia[‖], H.J. Gils[*], R. Glasstetter[**], C. Grupen[¶], A. Haungs[*], D. Heck[*], J.R. Hörandel[§], T. Huege[*], K.-H. Kampert[**], H.O. Klages[*], Y. Kolotaev[¶], H.J. Mathes[*], H.J. Mayer[*], C. Meurer[*], J. Milke[*], B. Mitrica[†], C. Morello[‖], G. Navarra[‡], S. Nehls[*], R. Obenland[*], J. Oehlschläger[*], S. Ostapchenko[*], S. Over[¶], M. Petcu[†], T. Pierog[*], S. Plewnia[*], H. Rebel[*], A. Risse[††], M. Roth[*], H. Schieler[*], O. Sima[†], M. Stümpert[§], G. Toma[†], G.C. Trinchero[‖], H. Ulrich[*], J. van Buren[*], W. Walkowiak[¶], A. Weindl[*], J. Wochele[*], J. Zabierowski[††], D. Zimmermann[¶],
KASCADE-Grande Collaboration
[¶] Fachbereich Physik, Universität Siegen, 57068 Siegen, Germany
[*] Institut für Kernphysik, Forschungszentrum Karlsruhe, 76021 Karlsruhe, Germany
[†] National Institute of Physics and Nuclear Engineering, 7690 Bucharest, Romania
[‡] Dipartimento di Fisica Generale dell'Università, 10125 Torino, Italy
[§] Institut für Experimentelle Kernphysik, Universität Karlsruhe, 76021 Karlsruhe, Germany
[‖] Istituto di Fisica dello Spazio Interplanetario, INAF, 10133 Torino, Italy
[**] Fachbereich Physik, Universität Wuppertal, 42097 Wuppertal, Germany
[††] Soltan Institute for Nuclear Studies, 90950 Lodz, Poland

***Abstract*— The KASCADE-Grande experiment, located at the site of Forschungszentrum Karlsruhe, Germany, studies cosmic radiation in the energy range 10^{14} eV–10^{18} eV. The data of the KASCADE array (0.04 km^2), one essential part of KASCADE-Grande, was used to analyse the chemical composition as well as the anisotropy of the cosmic radiation in the knee region of the energy spectrum. It was observed that the knee feature is caused by a decrease in flux of the light primaries leading to a heavier composition at energies above the knee. No anisotropies were observed in the KASCADE data. The sensitive detection area of KASCADE was enlarged to 0.5 km^2 by the Grande array to gain more statistics at higher energies around 100 PeV where the knee in the iron component of the cosmic radiation is expected. First results from analysis of air showers measured by KASCADE-Grande are presented.**

I. Introduction

In a large part, the origin of the cosmic radiation hitting the earth is still unknown. Its energy spectrum (figure 1) can be described by a simple power law $\propto E^{-\gamma}$, where a change of the spectral index at an energy of around 3 PeV from $\gamma \approx 2.75$ to $\gamma \approx 3.1$ is one pronounced feature, causing a sudden drop in cosmic ray flux. The explanation of this so called *knee* in the energy spectrum by cosmic ray studies is mandatory to solve the problem of the sources of high energetic cosmic rays. A popular model is, that at this energy the maximum acceleration by supernova remnants as cosmic ray sources is reached. The maximum energy $E_{\max} \propto Z \cdot R \cdot B$ is then a function of the charge Z of the cosmic ray particle. The parameters R and B refer to the size and the magnetic field of the acceleration region (see e.g. [12]). Therefore the knee should occur at higher energies with increasing charge

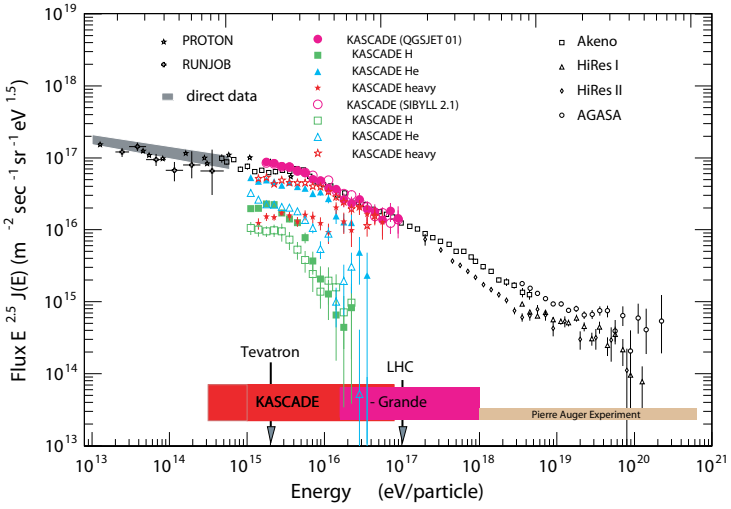

Fig. 1. All particle cosmic ray energy spectrum and the energy range covered by KASCADE-Grande.

Z. Other theoretic approaches predict instead a dependence on the atomic mass number A, as a result of interaction processes described by particle physics involving all nucleons of the cosmic ray nucleus. From these models follows that the knee in the energy spectrum of iron could be the origin of a possible second knee in the all particle energy spectrum. Therefore, a combined study of the energy spectrum and elemental composition is demanded to address these questions. Apart from the sources of cosmic radiation its propagation to earth is also still uncertain and some propagation models also predict a knee in the energy spectrum. An analysis of the anisotropy around the knee has to be performed to confirm or

exclude specific propagation models.

II. The KASCADE-Grande experiment

The KASCADE-Grande experiment depicted in figure 2 is a

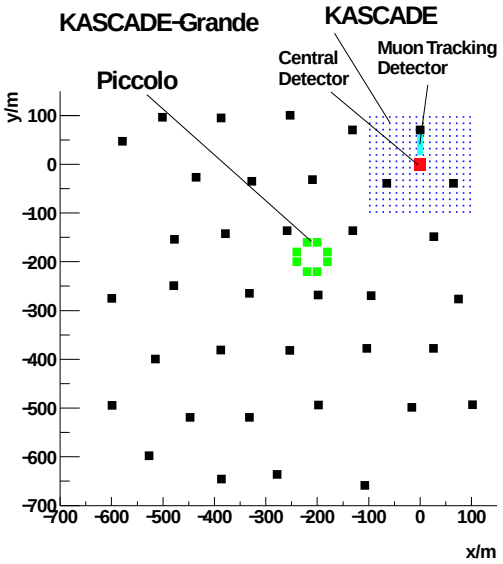

Fig. 2. Sketch of the KASCADE-Grande experiment showing the contributing parts.

multiple detector setup consisting of the KASCADE experiment [1] (see also figure 3), the trigger array Piccolo and the scintillator detector array Grande [15]. The KASCADE

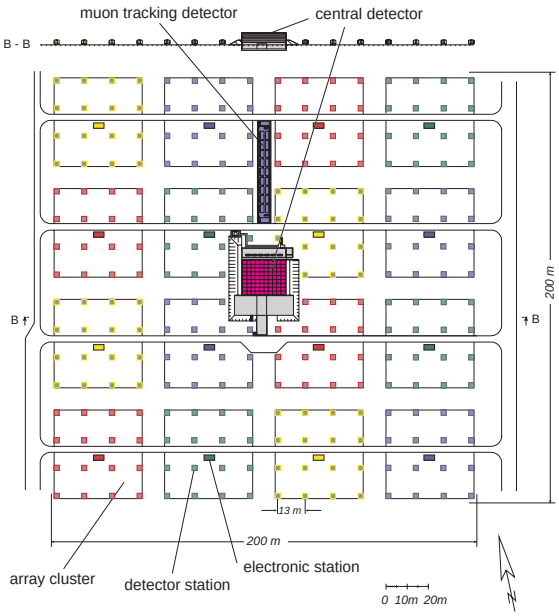

Fig. 3. Layout of the KASCADE experiment showing its subdetectors [1].

experiment is itself a multiple detector setup and its major parts are an array of 252 scintillator detector stations, a muon tracking detector and a central detector.

Most important for the analysis presented here are the two scintillator arrays: the KASCADE array and the Grande array, respectively. The Piccolo trigger array serves as a link between the Grande array and the KASCADE experiment and provides a trigger signal which is fast enough to trigger the muon detectors of the central detector.

The detector array of KASCADE is structured in 16 clusters as can be seen in figure 3. The detector stations of the 12 outer clusters house a detector for the electromagnetic as well as a detector for the muonic shower component. A separate determination of the electromagnetic and muonic shower size is therefore possible on a shower to shower basis. Showers having their core inside the central detector were of special interest for KASCADE to study as many shower characteristics as possible. The detector stations of the inner four clusters are therefore equipped with a detector for the electromagnetic air shower component only, because close to the shower core punch-through of the electromagnetic component makes an accurate determination of the muonic shower size impossible.

The Grande array is made up by 37 detector stations housing a scintillator of $10\,m^2$ sensitive area. Since there is no shielding of the detectors, they are only able to measure the charged shower component without separation into muons and electrons. In each station two types of photomultipliers are being operated with two different voltages. These two gain ranges assure a dynamic range which is big enough to measure single particles as well as high particle densities close to the shower axis.

III. Mass composition analysis

KASCADE data have been used to study the elemental composition of the primary cosmic radiation [4]. The basic data set for this analysis is represented by the two dimensional shower size spectrum measured by the KASCADE array, which is shown in figure 4. Each measured air shower enters

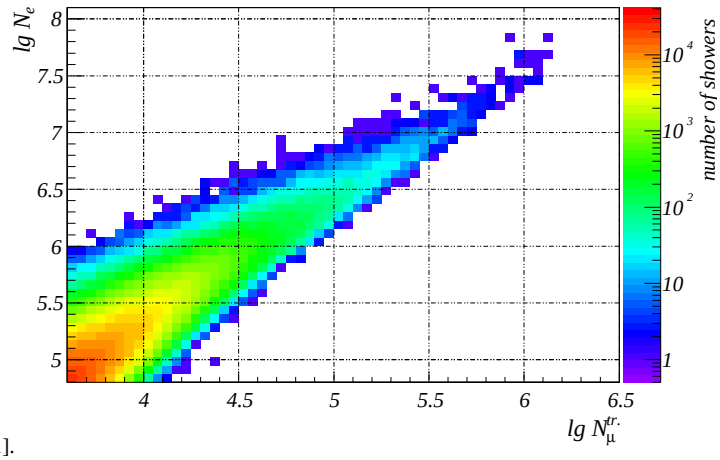

Fig. 4. The two-dimensional shower size spectrum of air showers measured by KASCADE [4].

this distribution with its measured number of electrons N_e

and its truncated number of muons N_μ^{tr}. The latter number corresponds to the number of muons with distances between 40 m and 200 m from the shower core, which prevents punch-through of the electromagnetic component close to the shower core biasing the measured muon size. About $6.9 \cdot 10^5$ events within the zenith angle interval $0° - 18°$ enter the distribution, corresponding to an effective measurement time of 900 days. The main cuts for the data are: distance of shower core from KASCADE center smaller than 91 m, shower age parameter of the fitted NKG function $0.2 < s < 2.1$, all array clusters were active, $\lg N_e \geq 4.8$ and $\lg N_\mu^{tr} \geq 3.6$. These cuts assure a good reconstruction quality and avoid threshold effects. The content of each cell N_i of the spectrum can be described by equation 1

$$N_i = C \sum_{A=1}^{N_p} \int_{-\infty}^{+\infty} \frac{dJ_A}{d \lg E} p_A(\lg N_{e,i}, \lg N_{\mu,i}^{tr} | \lg E) d \lg E. \quad (1)$$

The constant C is determined by the aperture and measuring time. The sum includes all primary types with mass A. The term p_A describes the probability that a primary of mass A and energy E initiates an air shower which is measured and reconstructed with shower sizes $\lg N_e$ and $\lg N_\mu^{tr}$ by KASCADE. This probability depends on natural phenomena like intrinsic shower fluctuations as well as on efficiencies of the experiment and the shower reconstruction accuracy which were studied and parametrized using Monte Carlo simulations performed with CORSIKA [11] 6.018 and the two high energy interaction models QGSJet [13] (2001 version) and SIBYLL [9] (version 2.1). In both cases GEISHA [8] (2002 version) has been used as low energy interaction model. The simulation has been limited to five primary particles H, He, C, Si and Fe as representatives for five mass groups. The integration over cell size and solid angle are not shown in equation 1 but are included in the analysis. The contents of all cells of the whole two-dimensional spectrum represent a system of coupled first order Fredholm integral equations, which can be solved by using of unfolding methods. The above mentioned parametrizations of the reconstructed Monte Carlo events are used to construct the response matrix. Slight changes to these parametrization allow to study systematic effects of the analyis. The results of the 2-dimensional unfolding procedure are depicted in figure 5 and 6 based on the QGSJet01 and SIBYLL model, respectively.

The results based on both interaction models show that the knee in the spectrum of primary cosmic radiation is caused by a decrease in flux of the light components and that the composition becomes thus heavier above the knee. Further, the positions of the knees in the single elemental group spectra indicate that a dependence on the charge Z is more probable than a dependence on the mass number A. The positions of the knee for both interaction models coincide within statistical errors as was found by fitting a power law parametrization to the all particle energy spectra based on both models. For QGSJet the knee position was measured at (4.0 ± 0.8) PeV

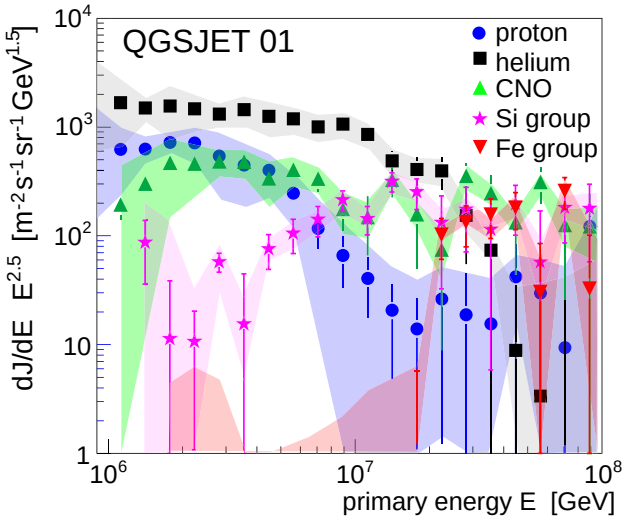

Fig. 5. Spectra of elemental groups resulting from the unfolding procedure based on the QGSJet01 model [4]. The shaded bands are estimates of the systematic uncertainties.

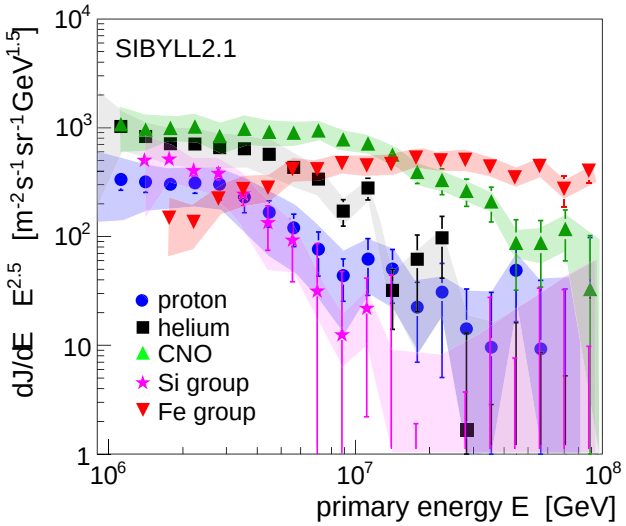

Fig. 6. Spectra of elemental groups resulting from the unfolding procedure based on the SIBYLL model [4]. The shaded bands are estimates of the systematic uncertainties.

and for SIBYLL at (5.7 ± 1.6) PeV.

By forward folding the obtained spectra and comparing the resulting two-dimensional size distribution with the measured one, significant differences caused by defficiencies of the interaction models are observed. None of the used interaction models is able to describe the measured data as can be seen in figures 7 and 8, where the differences are shown in terms of a χ^2 test.

A more detailed investigation of the $\lg N_e$ spectra in the region of $\lg N_\mu$ values with highest deviations is shown in figure 9 for the solution based on the QGSJet interaction model. The measured distribution is shown as points, the distribution resulting from the forward folding is shown as

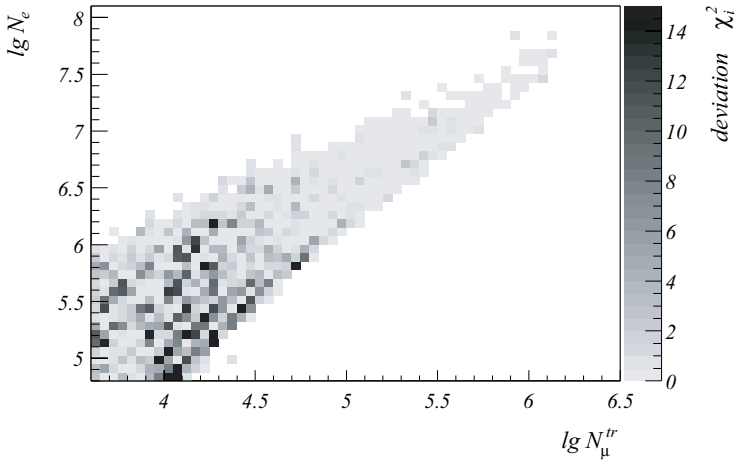

Fig. 7. Comparison between the measured size distribution and the forward folded elemental spectra obtained from unfolding the data based on the QGSJet01 model [4].

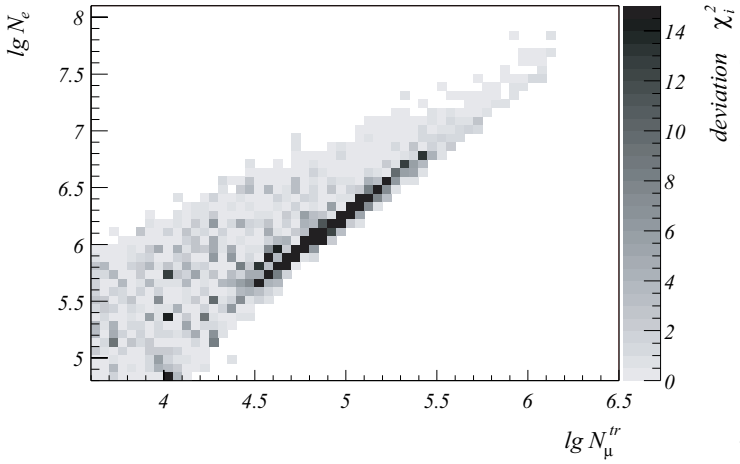

Fig. 8. Comparison between the measured size distribution and the forward folded elemental spectra obtained from unfolding the data based on the SIBYLL model [4].

histogram, and the contributions of the primary mass groups are shown as smooth curves. The heavy component (iron) is supressed as many showers from light primaries are needed to describe the right edge (large electron numbers) of the measured distribution. This behavior can be understood by the fact that the QGSJet model produces too many muons or too few electrons. At higher energies the description of the data by QGSJet improves. A similar analysis of the results based on the SIBYLL model yields that SIBYLL seems to overestimate the electron content or underestimate the muon number of air showers at higher energies.

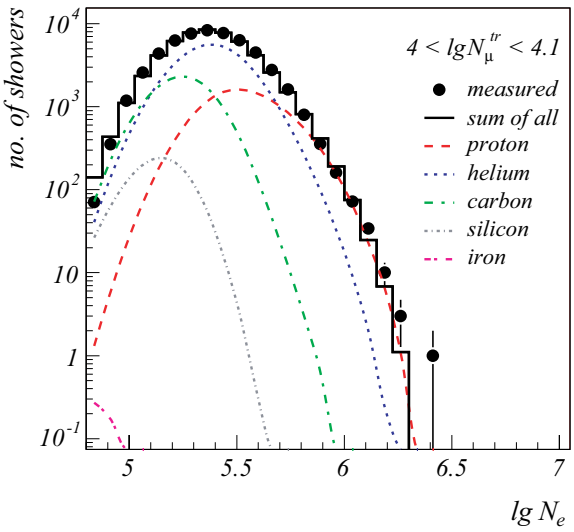

Fig. 9. Comparison of measured electron size distribution with QGSJet based solution for $4 < \lg N_\mu^{tr} < 4.1$ [4].

IV. Cosmic ray anisotropy around the knee

The analysis of anisotropies in the arrival directions of cosmic ray particles can give hints towards their sources and their propagation. Therefore, the KASCADE data taken between May 1998 to October 2002 were analyzed with respect to large and small scale anisotropies [2], [3]. In order to study the large scale cosmic ray anisotropy, the two-dimensional distribution of arrival directions of cosmic rays is reduced to the 1-dimensional right ascension distribution because of the small amplitudes expected from theory. The resulting right ascension distribution was analyzed by means of the Rayleigh formalism representing a first order approximation of the distribution's multipole expansion. To reduce contributions to the amplitudes by pseudo signals caused by variations of atmospheric ground pressure and temperature, the data is selected carefully and also corrected for these influences. The data is restricted to zenith angles below 40° (corresponding to a declination band $9° < \delta < 89°$). In this range KASCADE has an angular resolution of 0.55° for small showers and 0.1° for showers with electron numbers of $\lg N_e \geq 6$. Only sidereal days with continous data taking and a fully efficient (100 %) KASCADE array have been used. The latter requirement restricts the data to showers with electron numbers $\lg N_e > 4$. In total, 269 sidereal days of continous data taking entered the analysis, which has shown no significant Rayleigh amplitudes. Upper limits of the Rayleigh amplitudes were determined which are shown in figure 10. For comparison the predictions of various propagation models are drawn as well. The upper limits of the amplitude are in the range of 10^{-3} to 10^{-2}. These limits cannot restrict predictions by a diffusion-drift model taking into account a more complicated magnetic field distribution in our galaxy, but constrain calculations of a more simple leaky-

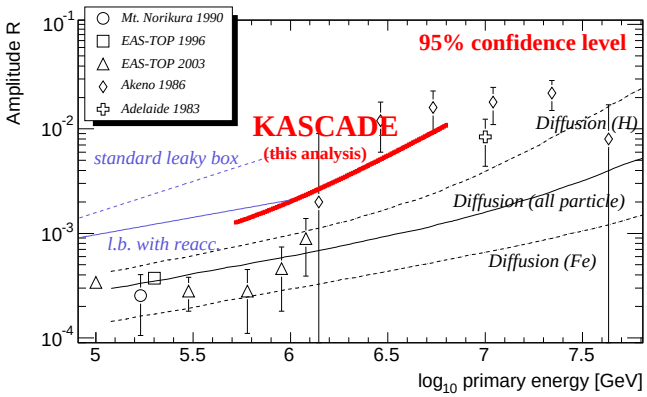

Fig. 10. Upper limits (95 %) on the large scale anisotropy determined by KASCADE [14].

box model (see [14] and references therein).

In order to study small scale anisotropies and possible point sources, the northern hemisphere seen by KASCADE (declination range $15° - 80°$) was separated into bins with a size optmized by Monte Carlo calculations to give maximum sensitivity to pointlike sources. The flux of cosmic radiation from each direction bin was compared to an artificially created isotropic background. This background was produced by applying the time shuffeling technique in which a measured air shower was given a new arrival direction either randomly chosen from the distribution of arrival directions of all measured showers or by taking the arrival direction of another measured air shower randomly chosen from the same data set. By the comparison the significance of flux excess is calculated for each direction bin. The resulting significances are summarized in a single distribution of significances which is shown in fig. 11.

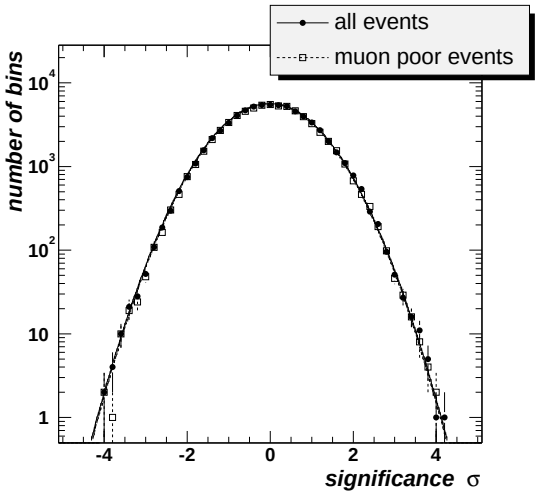

Fig. 11. Distribution of significances of the flux excess of all air showers and of candidates for gamma induced air showers (muon-poor events) [3].

The distribution shows no deviation from the Gaussian shape which means that no point source is being observed within the KASCADE data set used ($4.7{\cdot}10^7$ air showers). Neutral cosmic particles are the natural candidates to point back to their sources. The analysis was therefore repeated on muon-poor air showers which represent candidates for gamma induced air showers. No anisotropy has been observed with this data sample, too (fig. 11). Investigating in more detail the galactic plane or point source candidates like catalogized pulsars or supernova remnants neither showed any small scale anisotropy.

V. Reconstruction of Grande data

The KASCADE experiment observed a shift in the position of the knee with the primary particle group. While a knee could be observed in the light primary groups, the knee in the heavy component (*iron knee*) has not been detected, yet. The statistics of the KASCADE data in the region of the expected knee position at about 10^{17} eV is too low to state the position with an acceptable accuracy. In order to significantly increase the number of air showers measured at this high energy, the KASCADE experiment has been enlarged to 0.5 km^2 by the Grande detector field, an array of 37 scintillator stations with 10 m^2 sensitive area each.

As mentioned in section III the determination of energy spectra separated into different mass groups is based on the measured muon and electron numbers at ground. The detector stations of the Grande array, however, are not equipped with dedicated muon detectors, thus a direct measurement of the muon content of air showers measured by the Grande array is not possible. This information has to be reconstructed by using the information of the muon detectors of the KASCADE array. The KASCADE array offers in total 622 m^2 sensitive area for muons above an energy of 230 MeV and covers a radial range of maximal 280 m. To exclude misreconstructed showers having their core at the edge of the Grande array a circle with a radius of 250 m around the center of the Grande array is chosen as fiducial area [16]. This limits the radial range for a muon measurement by KASCADE to a core distance between 250 m and 530 m. The muon number is determined from the measured muon lateral distribution, which is described by

$$\rho_\mu = N_\mu \cdot f(r) \tag{2}$$

with

$$f(r) = \frac{0.28}{r_0^2}\left(\frac{r}{r_0}\right)^{p1} \cdot \left(1+\frac{r}{r_0}\right)^{p2} \cdot \left(1+\left(\frac{r}{10\cdot r_0}\right)\right)^{p3}.$$

The parameter $r_0 = 320$ m is kept fixed as well as the parameters $p1 = -0.69, p2 = -2.39$ and $p3 = -1.0$ which have been determined from simulated proton and iron air showers of energy 10^{16} eV and 10^{17} eV by fitting their muon lateral distributions with the parametrization given by equation 2 and averaging the fit results. The simulations have been obtained from CORSIKA using QGSJet [13] and FLUKA [6], [7] and high and low energy interaction models. In this way, the curvature of the lateral muon distribution is not varied and only the muon number is estimated according to $N_\mu = \sum_i n_i / \sum_i (f(r_i) \cdot A_i \cdot cos(\vartheta))$. Herein n_i is the number

of muons measured at distance r_i from the shower core within the area A_i. The parameter ϑ represents the measured zenith angle of the air shower.

A comparison between muon lateral distributions of reconstructed air showers measured by the Grande array and simulated proton and iron air showers for four different energy intervals in the zenith angle range $0° - 18°$ is shown in figure 12. The lines correspond to the parametrization (eqn. 2) with N_μ set to the measured mean muon number in each energy interval. The data is described well in the first two energy

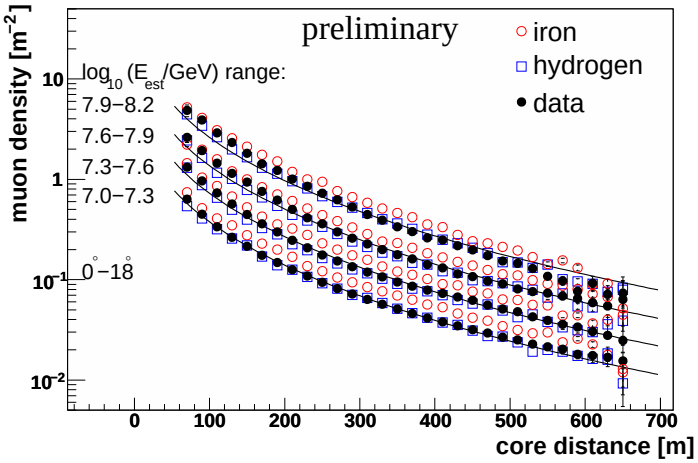

Fig. 12. Muon lateral distributions of measured and simulated air showers [16].

intervals. For higher energies an underestimation of the muon density on the order of 10 % can be observed for distances smaller than 200 m with the parametrization used. In the highest energy interval the used lateral function overestimates the muon density by 10 %–20 % at distances above 500 m. Investigation of higher zenith angle ranges shows that these deviations become smaller with increasing zenith angle.

The electron number of an air shower is reconstructed taking into account the estimated lateral density distribution of muons. In a negative-log-likelihood minimization core coordinates, arrival direction, electron number and shower age are determined using the particle densities and arrival times measured by the Grande detector stations. The minimization uses a modified NKG-function [5] to describe the measured particle densities corrected with the muon content taken from the estimated muon lateral density distribution.

With the possibility to reconstruct the muon content of air showers measured by Grande it is possible to produce the two-dimensional shower size distribution also for Grande, as can be seen in figure 13 for the zenith angle range $0° - 18°$. The dashed lines show an estimated primary energy. An analysis of the elemental composition analog to the analysis described in section III can thus be performed also for Grande shower data. Since the calibration of the KASCADE-Grande data collected so far is still being studied, the two-dimensional shower size spectrum can still slightly change. This and the still too low

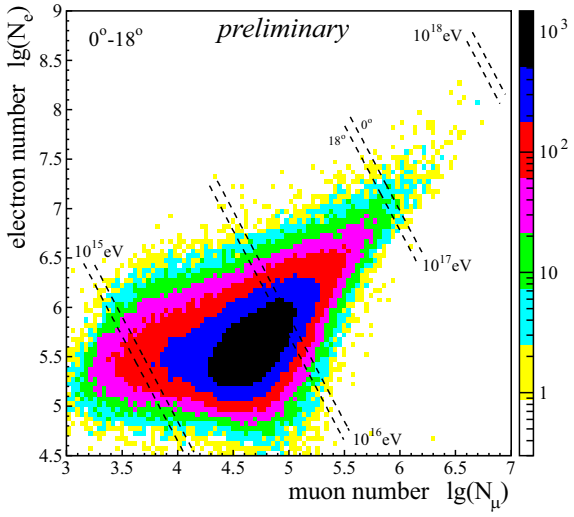

Fig. 13. Reconstructed electron and muon number distribution measured by KASCADE-Grande [10].

statistics are the reasons that no two-dimensional unfolding analysis has been performed yet.

Instead an energy spectrum has been determined by a 1-dimensional unfolding of the muon size spectrum measured by the Grande array, since the muon number is most sensitive to the primary energy. The resulting cosmic ray energy spectrum is shown in figure 14. The Grande data shown represent the

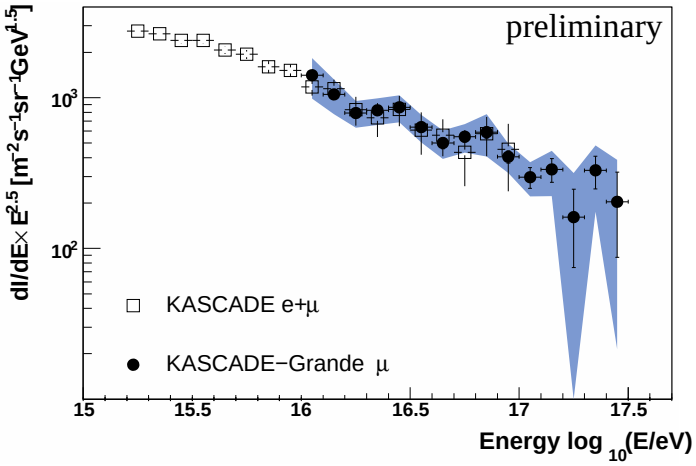

Fig. 14. Cosmic ray energy spectrum unfolded from the muon size spectrum measured with the Grande array compared to the energy spectrum from a 2-dimensional unfolding based on KASCADE data [16].

standard measurements of KASCADE-Grande in which both, the Grande array and the KASCADE array, respectively, took data simultaneously, which is mandatory to reconstruct the muon content of the air showers. The spectrum shows that with an effective data taking time of 363 days with KASCADE-Grande the same statistics has been collected as in 10 years data taking with KASCADE in the energy region given by the overlap of both spectra. The statistics is however still too small to draw conclusions about a second knee. So far no knee

structure is visible at higher energies in the energy spectrum.

VI. A FADC BASED DATA ACQUISITION SYSTEM

In order to improve the data quality of the data taken by the Grande detector stations, a Flash-ADC (FADC) based data acquisition system [17] is currently being commissioned. In each detector station digitization electronics will be installed, housing four interleaved 62.5 MHz FADCs with 12 bit resolution providing an effective sampling frequency of 250 MHz. While the FADCs sample the photomultiplier signals continously, a comparator triggers the readout of the digitized data from the FADC buffers, if the signal from the photomultiplier exceeds a programmable threshold. In this way, each detector station takes data self-triggered. The digitized data together with timing information of the measured event is transmitted over 700 m long optical fibers to the data acquisition station of the Grande array, where it is buffered by a receiver board to which up to eight Grande stations can be connected. Each board is connected to a first level PC via a PCI interface and transfers the digital data directly into its memory. A master PC scans the timing information in the data stored in the five PC-memories for shower coincidences and requests the full data of matching events only, to reduce the data transfer rate and the amount of data to be stored. Since the data is transferred optically it is not affected by possible sources of electric noise at the site of the Forschungszentrum Karlsruhe, which will increase the quality of the data acquired by the Grande array.

VII. SUMMARY

The two-dimensional shower size distribution measured by the KASCADE experiment was used to analyze the chemical composition of the primary cosmic radiation around the knee of the cosmic ray energy spectrum. An unfolding procedure was used based on simulations using CORSIKA with the two high energy interaction models QGSJet and SIBYLL. Five primary particle types H, He, C, Si, Fe have been used as representatives of different mass groups in the simulation. The results of the unfolding analysis show that, independent of the model used, the knee is caused by a decrease in flux of the light component and that the composition of cosmic radiation becomes heavier above the knee. The knee position was determined to be at (4.0 ± 0.8) PeV (QGSJet) or (5.7 ± 1.6) PeV (SIBYLL), respectively. A comparison between the measured data and the forward folded solution has revealed that both models have problems to describe the measured data in certain energy regions.

An analysis of the arrival directions of the measured air showers with respect to large and small scale anisotropies has been performed. To study the large scale anisotropy the right ascension distribution was investigated using the Rayleigh formalism. An upper limit of the Rayleigh amplitude has been determined to be in the range of 10^{-2} to 10^{-3}. No point-like source was found by looking for small scale anisotropies in the KASCADE data.

Investigations of the data taken by the whole KASCADE-Grande experiment have shown, that a reconstruction of the muon shower size is also possible for the showers measured by the Grande stations lacking a separate shielded muon detector. This reconstruction is achieved by making use of the muon detectors of the KASCADE experiment. Measured lateral density distributions are in agreement with simulations. A first energy spectrum has been unfolded using the muon size spectrum measured by KASCADE-Grande. The statistics is still too poor to draw conclusions about a knee at higher energies. A FADC based data acquisition system improving the data qualitiy is being commissioned.

ACKNOWLEDGMENT

The corresponding author would like to thank the organizers for an interesting and well organized symposium and a valuable time in Lisboa. KASCADE-Grande is supported by the Ministry for Research and Education of Germany, the INFN of Italy, the Polish State Committee for Scientific Research (KBN grant for 2004-06) and the Romanian Academy for Science, Research and Technology.

REFERENCES

[1] T. Antoni et al. - KASCADE Collaboration, *Nucl. Instr. Meth.* **A513** (2003) 429
[2] T. Antoni et al. - KASCADE Collaboration, *Astrophys. J.* **604** (2004), 687-692
[3] T. Antoni et al. - KASCADE Collaboration, *Astrophys. J.* **608** (2004), 865-871
[4] T. Antoni et al. - KASCADE Collaboration, *Astropart. Phys.* **24** (2005) 1-25
[5] W.D. Apel et al. - KASCADE Collaboration, *Astropart. Phys.* **24** (2006) 467-483
[6] A. Fasso, A. Ferrari, J. Ranft, and P.R. Sala, *CERN-2005-10, INFN/TC_05/11, SLAC-R-773* (2005)
[7] A. Fasso, et al., *Computing in High Energy and Nuclear Physics 2003 Conference (CHEP2003), La Jolla, CA, USA (paper MOMT005)* (2003), eConf C0303241 (2003), arXiv:hep-ph/0306267
[8] H. Fesefeldt, *Report **PITHA-85/02*** (1985), RWTH Aachen
[9] R.S. Fletcher, T.K. Gaisser, P. Lipardi and T. Stanev, *Phys. Rev.* **D50** (1994) 5710
[10] R. Glasstetter et al. - KASCADE-Grande Collaboration, *Proc. of 29^{th} ICRC Pune* (2005) 6, 293-296
[11] D. Heck et al., Forschungszentrum Karlsruhe, *Report FZKA 6019* (1998)
[12] A.M. Hillas, *J. Phys. G: Nucl. Part. Phys.* **31** (2005) R95
[13] N.N. Kalmykov and S.S. Ostapchenko, *Phys. Atom. Nucl.* **56** (1993) 346-353
[14] G. Maier et al. - KASCADE Collaboration, *Int. J. of Mod. Phys. A* **20** (2005) 29, 6840-6842
[15] G. Navarra et al. - KASCADE-Grande Collaboration, *Nucl. Instr. Math.* **A518** (2004) 207-209
[16] J. van Buren, *PhD thesis*, Karlsruhe, 2006
[17] W. Walkowiak et al. - KASCADE-Grande Collaboration, *IEEE Trans. Nucl. Sci.* **53** (2006) 265-269